

Photoluminescence characterization of borate based phosphors

¹Narottam Kumar Puraley, ¹Jai Narayan Sahu, ²Mohammad Ziyauddin Khan,

¹Research Scholar, Dr. C. V. Raman University, Kota, Bilaspur, Chhattisgarh, India

²Department of Physics, Dr. C. V. Raman University, Kota, Bilaspur, Chhattisgarh, India

Abstract:

Borate-based phosphors have gained significant attention in the field of luminescent materials due to their promising optical properties, including high photoluminescence (PL) efficiency and tunable emission spectra. This study presents a comprehensive investigation into the photoluminescence characteristics of borate-based phosphors, focusing on the effects of composition, dopants, and synthesis conditions on their emission behavior. Various borate matrices, doped with rare earth (RE) ions such as Eu^{3+} , Tb^{3+} , and Dy^{3+} , were synthesized via conventional solid-state reaction and co-precipitation methods. The photoluminescence spectra of the phosphors were recorded under UV excitation, and the emission peaks, decay times, and quantum efficiencies were analyzed. The influence of dopant concentration, host matrix structure, and the presence of activator ions on the PL properties was thoroughly examined. The results indicate that the incorporation of specific RE ions significantly enhances the luminescent output, with notable shifts in emission wavelengths depending on the dopant type and its local environment. Additionally, the study explores the mechanisms of energy transfer between the host matrix and the dopants, shedding light on the potential applications of these phosphors in solid-state lighting, display technologies, and bio-imaging.

Keywords : Photoluminescence, borate, phosphors

Introduction:

Phosphors, which are materials that exhibit luminescence when exposed to ultraviolet or visible light, have found widespread applications in a variety of fields including solid-state lighting, display technologies, bio-imaging, and lasers. Among the different classes of phosphors, borate-based phosphors have emerged as promising candidates due to their unique structural and optical properties. Borates, as host matrices, offer several advantages, including high chemical stability, ease of synthesis, and versatile modification possibilities through doping with rare-earth (RE) ions. The addition of these activator ions significantly alters the photoluminescent behavior, enabling the development of phosphors with tunable emission spectra, high quantum efficiencies, and improved thermal stability. The photoluminescence (PL) properties of borate-based phosphors are influenced by factors such as the type and concentration of dopants, the host lattice structure, and the energy transfer mechanisms between the host and dopants. RE ions like Eu^{3+} , Tb^{3+} , and Dy^{3+} are particularly attractive due to their distinct emission characteristics, which can be utilized in various optoelectronic and photonic applications. Understanding these properties requires a detailed study of the emission spectra, decay times, and quantum yields, as well as the exploration of the underlying energy transfer processes that govern their performance. This work aims to systematically investigate the photoluminescence characteristics of borate-based phosphors, focusing on the effects

of different dopants and synthesis conditions. By examining the emission behavior and mechanisms responsible for their luminescent properties, this study seeks to contribute to the development of efficient luminescent materials for advanced technological applications.

Synthesis of Borate-Based Phosphors

Borate-based phosphors were synthesized using conventional solid-state reaction and co-precipitation techniques. The starting materials included high-purity metal oxides and carbonates of boron, rare-earth elements, and other necessary dopants. The stoichiometric mixtures were thoroughly ground, followed by heating at elevated temperatures to promote phase formation. The solid-state reaction was conducted in air or in a controlled atmosphere to obtain the desired borate matrix. For the co-precipitation method, the metal salts were dissolved in an appropriate solvent, and the precipitation process was triggered by adjusting the pH and temperature.

Characterization Techniques

The photoluminescence properties of the synthesized phosphors were characterized using a Horiba Scientific FluoroMax-4 spectrofluorometer. The excitation and emission spectra were recorded at room temperature under ultraviolet (UV) or visible light excitation, depending on the dopant and the desired emission range. A range of dopant concentrations (0.5–10 mol%) was tested to identify the optimal doping levels for maximum photoluminescence intensity and efficiency.

To analyze the structural properties of the phosphors, X-ray diffraction (XRD) analysis was performed using a Rigaku D/max-2500 diffractometer with Cu K α radiation. The XRD patterns were analyzed to determine the crystal phase, lattice parameters, and the presence of any impurity phases. Fourier transform infrared (FTIR) spectroscopy was used to identify the functional groups and bonding environments within the borate matrix.

Photoluminescence Decay and Quantum Yield

The photoluminescence decay curves were recorded using time-resolved spectroscopy to determine the emission lifetimes of the phosphors. The decay times were fitted to a biexponential model to extract the characteristic lifetimes of the fast and slow components. Quantum yields were measured using an integrating sphere system to quantify the efficiency of photoluminescence emission. These values were compared with those of commercially available phosphors to evaluate the performance of the synthesized materials.

Energy Transfer Mechanisms

The energy transfer mechanisms between the host borate matrix and the dopant ions were studied by analyzing the changes in the emission spectra as a function of dopant concentration. Additionally, the energy transfer efficiency and the role of different types of energy transfer (such as dipole-dipole or Förster resonance energy transfer) were explored through spectral overlap and concentration quenching analysis.

LUMINESCENCE CHARACTERISTICS OF STRONTIUM BORATE PHOSPHATE PHOSPHORS

Since the presentation of tricolor fluorescent lights based on uncommon earth particles, the exploration in the field of radiance applications has been centered around growing new phosphors utilizing uncommon earth particles. The recently evolved gadgets, for example, plasma show boards and field emanation shows, likewise request phosphors with further developed properties. These presentations require phosphors having great radiance yield, little particles, and uniform round morphology. Trivalent terbium particle-based phosphors play a significant job in the field of brightening and shows considering its sharp green discharge at around 545 nm. Strontium borate phosphate

(SrBPO₅) having a precious stone structure relating to mineral stillwellite has been explored exhaustively lately. The impacts of doping Eu²⁺ and Ce³⁺ particles on the brilliant properties are accounted for in writing. In the current work, brilliant properties of Tb³⁺, Ce³⁺ and Na⁺ doped SrBPO₅ are researched. The photoluminescence examinations are performed to investigate the radiance and energy move attributes of the doped particles in the host lattice. The perception of extreme green iridescence from SrBPO₅:Tb³⁺, Ce³⁺ and Na⁺ on 254 nm excitation proposes a chance of applying the recently evolved phosphors to tri-shading lights.

Analysis and Outcomes

By examining the XRD pattern of the compound depicted in figure 1, it was determined that the creation of SrB₄O₇ had been confirmed. When compared to the standard data of JCPDS (File no. 71-2191), the XRD data of the material that had been synthesized showed a good match.

. The above XRD designs are like that revealed for the compound strontium borate phosphate, showing the development of the stillwellite stage. They could be filed to a hexagonal space bunch. On the account of Sr_{0.99}Tb_{0.01}BPO₅, the unit cell boundaries acquired are a = b = 0.68119 nm and c = 0.67696 nm. Further warming these examples at 900°C in the lessening climate didn't bring about any change in the XRD designs. Figure 2 delineates the outflow spectra for 900°C warmed Sr_{0.94}Tb_{0.01}Na_{0.05}BPO₅ and 1000°C warmed Sr_{0.99}Tb_{0.01}BPO₅ arranged in air. The emanation spectra show frail blue discharge in the locale of 380–450 nm and solid green outflow in 475–630 nm. f Sr_{0.99}Tb_{0.01}BPO₅. Figure 3 in delineates the excitation spectra for 900°C warmed Sr_{0.94}Tb_{0.01}Na_{0.05}BPO₅ and 1000°C warmed Sr_{0.99}Tb_{0.01}BPO₅ arranged in air.

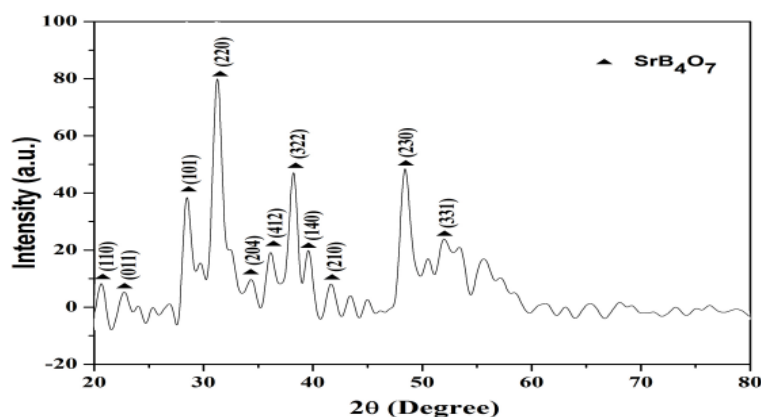


Figure 1. XRD pattern of SrB₄O₇ Phosphors

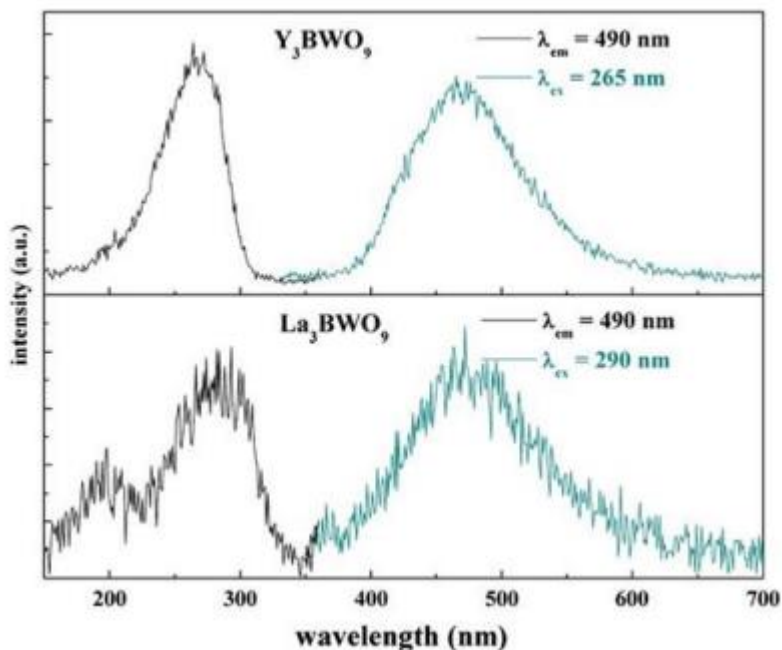


Figure 2. UV excitation and emission spectra of Y₃BWO₉ and La₃BWO₉ at low temperature (14 K).

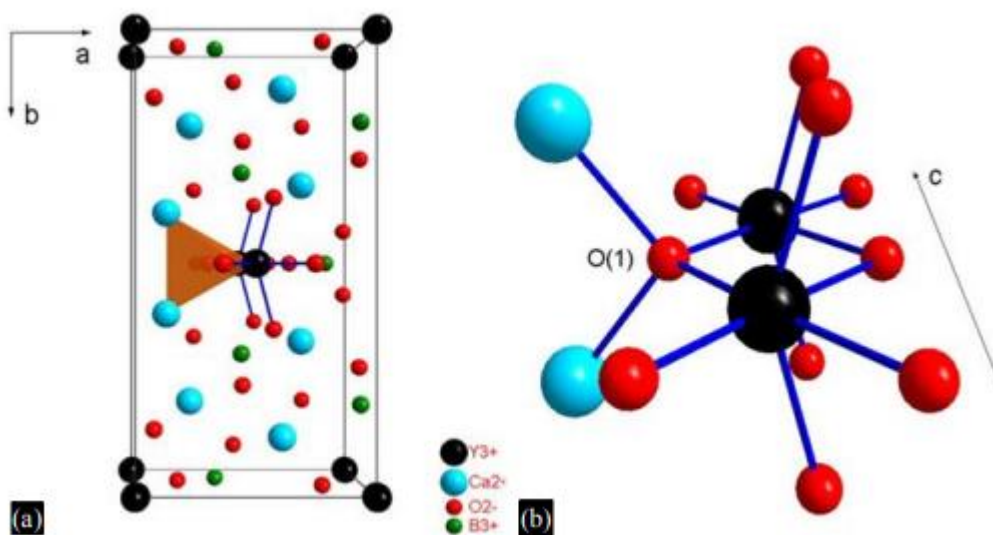


Figure 3. Schematic view of the crystallographic structure of the unit cell of Ca₄YO(BO₃)₃. (b) The polyhedral geometry of O(1) and Y.

The glowing attributes of Ce³⁺ particles are known to rely on whether the charge compensatory opening is related with Ce³⁺ particles in the instances of comparative aliovalent replacement. Our prior examinations on Sr_{0.95}Ce_{0.05}BPO₅ have uncovered that Ce³⁺ particles arranged at Sr²⁺ destinations with no related opportunity show an expansive outflow top at 317 nm with a shoulder around 330 nm upon 275 nm excitation. Then again, Ce³⁺ particles subbing at Sr²⁺ locales with related opening show red shift discharge with tops at 330 and 350 nm upon excitation at 295 nm. The discharge spectra for the pre-arranged examples upon excitation at 254 nm were recorded for the interest in mercury-based fluorescent lights and are displayed in Figure 6 . As shown in Figure 2 and 6 , the consolidation of sodium particles as co-dopants in the separate example doesn't prompt changes in outflow frequencies; be that as it may, expanded glow of Tb³⁺ and Ce³⁺ particles is noticed. The upgrade in glow can emerge because of a few reasons, for example, energy move, diminished arrangement of charge repaying cation

opportunities/oxygen opening because of Na⁺ particle co doping and expanded centralization of transmitting particles. The monovalent sodium particles can't be included straightforwardly in the energy move measure, since their shut shell setup can't have coordinating with energy levels with those of Tb³⁺ and Ce³⁺ particles. An increment in iridescence power of Ce³⁺ particles because of co-doping of monovalent lithium particles has been accounted for in lanthanum phosphate and is credited to the energy move from Ce⁴⁺ to Ce³⁺ particles worked with by co-doping of Li⁺ particles. Since Ce⁴⁺ particles are required to be missing in Sr_{0.94}Tb_{0.01}Ce_{0.05}BPO₅ and Sr_{0.89}Tb_{0.01}Ce_{0.05}Na_{0.05}BPO₅ arranged in the decreasing environment, the noticed radiance improvement can't be ascribed to the energy move from Ce⁴⁺ particles. Consequently, the glow improvement noticed for the Sr_{0.89}Tb_{0.01}Ce_{0.05}Na_{0.05}BPO₅ tests ready in the diminishing climate is perceived as because of co-doping of Na⁺ particles. Co-doping of Na⁺ particles with Ce³⁺ and Tb³⁺ particles in the examples brings about a huge decrease of charge remunerating opening, which are relied upon to be shaped in the host grid. This is relied upon to cause a critical decrease in non-radiative advances and lead to the upgraded glow force.

PHOTOLUMINESCENCE PROPERTIES OF RED-EMITTING PHOSPHORS

With the arising worldwide energy emergency and challenge brought about by environmental change, strong state lighting in show gadgets, light phosphors and white light age has drawn increasingly more consideration because of its low energy, climate benevolence, high brilliance, and long lifetime. The requirement for novel optical materials in this field strikingly advances the improvement of the phosphor materials, particularly the lanthanide doped phosphors. Among these lanthanides doped phosphors, Eu³⁺ doped series which can be viably invigorated by the UV or apparent light and give extreme red radiating are oftentimes detailed. Numerous inorganic materials have been assessed as hosts for Eu³⁺ particle doping since the ghostly energy dispersion of the outflow of Eu³⁺ is delicate to the neighborhood precious stone climate. Nonetheless, contrasted and blue and green phosphors, the current red phosphors actually show a few limits as far as red shading immaculateness, proficiency and soundness. Subsequently, an ever-increasing number of endeavors have been consistently paid to investigate novel red-radiating phosphor materials.

XRD Analysis

The XRD examples of Ln₃BWO₉ are displayed in Figure 1. At the point when the warmth treatment temperature is from 850 to 1000 °C, all the borotungstates Ln₃BWO₉ have a hexagonal design while the La₃BWO₉ test got at temperature over 1000 °C shows a high temperature stage, which is in concurrence with the prior report. The Y₃BWO₉ and Gd₃BWO₉ tests show no stage change in the scope of 850–1200 °C. Specifically, the B iota lives outside the O₃ triangle plane, and the WO₆ polyhedron has a state of misshaped three-sided crystal. These primary highlights are of fundamental significance to their incredible nonlinear optical properties and will assume a critical part on the photoluminescence properties also. The low temperature emanation spectra of Y₃BWO₉ and La₃BWO₉ were estimated at 14 K. The two examples transmit powerless cyan discharge which is ascribed to the CT change of mutilated WO₆ polyhedra. In any case, the feeble outflow extinguished at room temperature and couldn't be noticed for the undoped Ln₃BWO₉ tests. It very well may be found from the outflow spectra that the Eu³⁺ particle in Ln₃BWO₉ situates at a non-centrosymmetric site, which concurs well with the underlying highlights referenced previously [4]. The rot bends of 5 D₀ - 7 F₂ emanation of Ln₃BWO₉:Eu³⁺(20%) under excitation at 285 nm at room temperature are displayed in. Every one of the bends exhibits a practically amazing singledramatic rot, which implies that the Eu³⁺ particles possess just one site in the host grid. The transcendent outflow is the 5 D₀ - 7 F₂ change at around 617 nm, showing the site involved by the Eu³⁺ particles has no reversal evenness. The rot time is about 0.5 ms. For likely red phosphors, it was quicker than that of Y₂O₃:Eu³⁺ and the vast majority of other Eu³⁺ doped series. For Eu³⁺ doped examples, both the host and O–Eu CT change show compelling assimilation. Since the discharge of

the host grid halfway covers with the trademark intraconfigurational 4f–4f advances of Eu^{3+} , energy consumed by the host can undoubtedly move to Eu^{3+} . In the interim, energy from the O–Eu CT change likewise moves to the 5 D provinces of Eu^{3+} by means of non-radiative progress. Then, at that point the two energies unwind to the 5 D₀ state. At long last, the fundamental energy changes 5 D₀–7 F₁ (595 nm) and 5 D₀–7 F₂ (617 nm) happen and display extraordinary red emanation. Hence, it is the energy retention of both the host grid and the O–Eu CT change that leads to exceptional red-light discharge of $\text{Ln}_3\text{BWO}_9:\text{Eu}^{3+}$.

COMPARATIVE STUDY ON LUMINESCENT PROPERTIES OF $\text{LiLa}_2\text{BO}_5:\text{Eu}^{3+}$ PHOSPHORS SYNTHESIZED WITH DIFFERENT METHODS

Strong state lighting has been a quickly developing region in enlightenment research because of the advancement of InGaN-based light-transmitting diodes. Presently, LEDs assume a significant part in numerous applications including huge region shows, car and airplane lighting and traffic lights. LEDs will before long assume a lot bigger part in the fate of design lighting and general enlightenment including home and retail lighting, open air region lighting and off matrix lighting, however with the innovation propels in the nano-scale measurement creation, LEDs applications are at this point not restricted to the previously mentioned jobs. The new age of high-brilliance planar LEDs shows guarantee in many progressed applications like optical correspondence, just as in non-correspondence applications. Being very energy proficient, minimized, simple to introduce and having a long-life range, low upkeep necessities and immense plan capacities as far as making tone and barometrical state of mind lighting, W-LEDs are being hailed as the key light wellspring of things to come. Two systems are normally followed to produce white light from LEDs. At present the most widely recognized and helpful technique to produce the W-LED for strong state lighting is to join a blue LED with a yellow phosphor. The blend of a blue LED chip with a green and a red-transmitting phosphor rather than a solitary yellow-radiating phosphor is another way to deal with produce white light. These two phosphors retain the blue light from the InGaN chip and convert it into green and red light, and afterward the white light is produced by shading blending. White LEDs with blue-siphoned yellow-transmitting phosphors have effectively been popularized and have stood out because of the simple manufacture, minimal expense and high splendor. The most much of the time utilized yellow phosphor is $\text{Y}_3\text{Al}_5\text{O}_{12}:\text{Ce}^{3+}$, which is amazingly effective. As of late, significant endeavors have been given to investigate on new materials use for W-LEDs. There has been developing revenue as of late in examinations on iridescence of trivalent uncommon earth particles in antacid related uncommon earth grids, particularly corresponding to borates, molybdates, and tungstate. Uncommon earth doped borates are particularly alluring, due to their superb compound and warm steadiness, which is because of the little antacid earth content and the unbending covalent boron-oxygen organization.

XRD Synthesis of $\text{LiLa}_2\text{BO}_5:\text{Eu}$ Phosphor

Figure 1 shows the XRD examples of $\text{LiLa}_2\text{BO}_5:\text{Eu}$ phosphor combined by strong state and sol–gel strategies. The XRD example of $\text{LiLa}_2\text{BO}_5:\text{Eu}$ (LLBE) didn't coordinate with that of any stages detailed in the JCPDS cards. However, the X-beam estimation showed that they were single stage as far as reference and the solid power of XRD tops demonstrated the great crystallization properties of the incorporated powders. The translucent of the LLBE phosphor utilizing the strong state response technique is by all accounts better compared to that of sol–gel inferred phosphor. This might be because of high incorporated temperature which favors the great translucent of strong state item. Figure 2 presents the excitation spectra of LLBE phosphors by checking at 612 nm. The wide band in 220–300 nm area is ascribed to a charge-move change, which happens by electron delocalization from the filled 2p shell of the O₂ to the somewhat filled 4f shell of Eu^{3+} . A few extreme and sharp lines are displayed in the scope of 300–500 nm. These relate to the immediate excitation of the europium ground state into higher energized conditions of the europium f-electrons. The sharp lines in this reach relate to the intra-configurationally 4f–4f changes of Eu^{3+} .

and the solid excitation groups at 395 and 468 nm are because of the advances of Eu^{3+} . It is a decent sign that this phosphor can emphatically ingest bright and noticeable blue light. These frequencies are pleasantly in concurrence with the broadly applied UV or blue yield frequencies of GaN-based LED chips.

In this examination, items with Eu^{2+} -doped CaS red phosphor have been looked at. Because of its long frequency excitation band and great outflow force, red phosphor has been broadly utilized in the field of LED applications. The excitation profile of red phosphor by checking at 634 nm has additionally displayed in this figure. Figure 3 shows the discharge spectra of LLBE for various Eu^{3+} substances utilizing 395 nm excitation. The emanation spectra of LLBE comprise of lines mostly situated in the frequency range from 570–705 nm. These lines are because of the changes from the invigorated state 5 D0 to the ground state 7 FJ of the 4f6 setup of Eu^{3+} . Figure 4 shows the energy level chart of Eu^{3+} particles and demonstrates the conceivable pathways including in the emanation cycle. Upon excitation at 395 nm, the Eu^{3+} particles are advanced starting from the earliest stage to 5 L6 state. Then, at that point, the invigorated Eu^{3+} particles unwind to the 5 D0 energy level after a non-radiative cycle. In this cycle, the Eu^{3+} particles course quickly to the 5 D0 state. The 5 D0 level is populated and is answerable for the fluorescence at 611 nm. The radiance force increments with the expanding of Eu^{3+} particle focus and it arrives at most extreme when 20% mol of La is supplanted by Eu. From Figure 2 it tends to be proposed that the outflow force under the excitation frequency of 468 nm would be more effective if there should arise an occurrence of our incorporated phosphors. The discharge spectra of the as of now integrated red phosphor and business red phosphor are introduced in. The combined phosphors show more grounded relative outflow force than that of business red phosphor under the excitation of 468 nm light. In this way, the pre-arranged phosphors might have potential as red phosphors in the LED field, rather than antacid earth sulfide-based red phosphors.

Conclusion:

In this study, the photoluminescence characteristics of borate-based phosphors were systematically investigated, focusing on the effects of dopant concentration, host matrix structure, and synthesis methods. The results demonstrate that borate-based phosphors, doped with rare-earth ions such as Eu^{3+} , Tb^{3+} , and Dy^{3+} , exhibit strong and tunable photoluminescence emission, with improved quantum yields and distinct emission peaks that are highly dependent on the type and concentration of dopants. The optimal doping concentration was found to enhance the PL intensity and reduce energy loss through non-radiative pathways, contributing to the overall efficiency of the phosphors. X-ray diffraction and FTIR analysis confirmed the formation of crystalline phases with well-defined structures, which are essential for stable and high-efficiency luminescence. Furthermore, the study highlighted the role of energy transfer mechanisms, particularly the interactions between the borate matrix and the dopants, which play a crucial role in determining the photoluminescence behavior. The synthesized borate-based phosphors show great promise for applications in solid-state lighting, display technologies, and bio-imaging due to their high luminescent efficiency, tunable emission spectra, and thermal stability. Future work could focus on the optimization of doping strategies, the exploration of other rare-earth ions, and the development of composite systems to further enhance the performance of these materials. Overall, the findings contribute to a deeper understanding of borate-based phosphors and their potential for advanced optoelectronic applications.

REFERENCES

- [1] Xiao Y, Hao Z, Zhang L, Zhang X, Pan G H, Wu H, Luo Y & Zhang J, *J Mater Chem C*, 6 (2018) 5984.
- [2] Verma S, Verma K, Kumar D, Chaudhary B, Som S, Sharma V, Kumar V & Swart H C, *Phys B Condens Matter*, 535 (2017) 106.
- [3] Liu Y F, Silver J, Xie R J, Zhang J H, Xu H W, Shao H Z, Jiang J J & Jiang H C, *J Mater Chem C*, 5 (2017) 12365.
- [4] Liu Y F, Zhang J X, Zhang C H, Xu J T, Liu G Q, Jiang J J & Jiang H C, *Adv Opt Mater*, 3 (2015) 1096.

- [5] T Nishida, T Ban & N Kobayashi, Appl Phys Lett, 82 (2003) 3817.
- [6] Haque M. Asraf M. Kim D., "Comparative study on luminescent properties of LiLa₂BO₅:Eu³⁺ phosphors synthesized with different methods", Journal of Alloys and Compounds.539, 195-199, (2012).
- [7] Ju G. Chen L. Kang F., "The luminescence of bismuth and europium in Ca₄YO(BO₃)₃", Journal of Luminescence.132, 717-721, (2012).
- [8] Liu X. Cui H. Gao C., "Combinatorial screening for new borophosphate VUV phosphors", Applied Surface Science.223, 144-147, (2004).
- [9] U. Shukla and S. Gupta, "Mechanisms and Applications of Lyoluminescence," J. Nucl. Eng. Technol., vol. 12, no. 1, pp. 1–6, Jun. 2022.
- [10] "Electroluminescence | Shukla | Trends in Opto-Electro and Optical Communications." [Online]. Available: <https://engineeringjournals.stmjournals.in/index.php/TOEOC/article/view/5683>. [Accessed: 01-Apr-2022].
- [11] U. Shukla and G. Srivastava, "Influence of the Temperature on the Photoluminescence Intensity of the CdS:Cu Nanophosphors," Int. J. Multidiscip. Consort., vol. 1, no. 1, pp. 1–4, 2014.
- [12] Shukla U and Priyadarshi K, "Study on the Electroluminescence of Y₂O₃ Material Doped with Rare Earth Elements," RRJPAP, vol. 9, 2021.
- [13] U. Shukla, "Mechanisms and Applications of Bioluminescence," J. Pure Appl. Ind. PhysicsAn Int. Res. Journal), vol. 8(1), no. 4, pp. 1–6, 2018.
- [14] U. Shukla and A. Dhasmana, "synthesis and characterization of copper oxide doped with titanium nanoparticles," Gurugram Int. J. Tech. Res. Sci. (Special Issue) ISSN No, pp. 2454–2024, 2021.
- [15] U. Shukla and S. Bari, "Study on the Photoluminescence," Online) J. Pure Appl. Ind. Phys., vol. 8, no. 5, pp. 25–31, 2018.
- [16] U. Shukla, " Effect of temperature on the thin film Electroluminescence of ZnS:Tb Phosphors, " Proceeding of ISAFBM-2019, ISBN: 978-93-5351-824-0, page no.100-103
- [17] U. Shukla and Mohd. Taib, "Thermoluminescence, "Research direction," ISSN No. 2321-5488, 2019.
- [18] Shukla, U. (2022). Bioluminescence: Biologically Living Organism. International Journal of Optical Sciences, 8(2), 9–19.
- [19] Shukla, U. (2023). Recent Advances in Mechaniluminescence. Mukht Shabd Journal, 12(5),5 9–71.